Electron-stimulated desorption of cesium atoms from cesium layers adsorbed on gold-covered tungsten

Electron-stimulated desorption of cesium atoms from cesium layers adsorbed on gold-covered tungsten

V N Ageev, Yu A Kuznetsov and N D Potekhina

A F Ioffe Physico-Technical Institute, Russian Academy of Sciences, 194021,
St Petersburg, Russia

E-mail: kuznets@ms.ioffe.ru

Abstract
The electron-stimulated desorption (ESD) yields and energy distributions (ED) for neutral cesium atoms have been measured from cesium layers adsorbed on a gold-covered tungsten surface as a function of electron energy, gold film thickness, cesium coverage and substrate temperature. The measurements have been carried out using a time-of-flight method and surface ionization detector in the temperature range 160–300 K. A measurable ESD yield for Cs atoms is observed only after deposition of more than one monolayer of gold and cesium on a tungsten surface at a temperature $T = 300$ K, which is accompanied by the formation of a CsAu semiconductor film covered with a cesium atom monolayer. The Cs atom ESD yield as a function of incident electron energy has a resonant character and consists of two peaks, the appearance of which depends on both electron energy and substrate temperature. The first peak has an appearance threshold at an electron energy of 57 eV and a substrate temperature of 300 K that is due to Au $5p_{3/2}$ core level excitation in the substrate. The second peak appears at an electron energy of 24 eV and a substrate temperature of 160 K. It is associated with a Cs 5s core level excitation in the Cs adsorbed layer. The Au $5p_{3/2}$ level excitation corresponds to a single broad peak in the ED with a maximum at a kinetic energy of 0.45 eV at a substrate temperature $T = 300$ K, which is split into two peaks with maxima at kinetic energies of 0.36 and 0.45 eV at a substrate temperature of 160 K, associated with different Cs atom ESD channels. The Cs 5s level excitation leads to an ED for Cs atoms with a maximum at a kinetic energy of ∼0.57 eV which exists only at $T < 240$ K and low Cs concentrations. The mechanisms for all the Cs atom ESD channels are proposed and compared with the Na atom ESD channels in the Na–Au–W system.

This paper is devoted to the memory of Professor T E Madey—an excellent man and brilliant scientist, who made great contributions to the study of ESD.

1. Introduction

The electron-stimulated desorption (ESD) of ions and neutral particles from the surface of solids is used to analyze and modify adsorbed layers [1–3]. In this phenomenon the desorbing particles are obtained by transformation of the potential energy of an electronic excitation localized near the particle–surface bond into the kinetic energy of the desorbing particles. So its study may give new information on excitation states of the electronic system and on the ESD mechanism. In most cases the main component of the ESD flux are neutral particles but there is a shortage of reliable measurements of the ESD yield and energy distribution for neutral particles [4]. However, the study of the ESD for neutrals revealed a great variety of excited electronic states of solids and the desorption channels as a result of the decay of these excitations [5–14]. In particular, the ESD yield for neutrals from some adsorbed systems shows resonant-like peaks at electron energies which correlate well with the substrate core level excitation energies. Such peaks are observed in the ESD yield for alkali-metal atoms from alkali-metal layers adsorbed on oxidized molybdenum [6–8] and in

the ESD yield of Eu and Sm atoms from rare-earth metal layers deposited on oxidized tungsten [9, 10] as a function of electron energy. We have recently measured similar resonant-like peaks in the Cs atom ESD yield from a cesium layer adsorbed on a germanium thin-film-covered tungsten [11, 12] and in the Na atom ESD yield from a sodium layer deposited on gold-covered tungsten [13, 14] as a function of electron energy.

The ESD yield from metal-film systems is usually negligible because of the small excitation lifetime in such systems. However, the deposition of an insulating or semiconductor film (even of monolayer thickness) between the substrate and adsorbed metal hinders electron exchange between these layers and the ESD yield of atoms increases by a large factor [1].

A striking example of this phenomenon gives the Na and Cs adsorption on a gold-film-covered tungsten surface [13, 14]. Until the Au and Cs coverage does not exceed one monolayer the system represents a metal with an adsorbed Cs layer. But when the Au and Cs coverage becomes more than one monolayer a semiconductor CsAu compound starts to grow between the Cs and Au monolayers. Then irradiation of the surface with electrons can lead to desorption of Cs atoms from the Cs monolayer parts that have been formed on the surface of this compound but not those from an uncovered gold layer [15]. The evidence of ionic CsAu semiconductor formation with an energy gap of 2.6 eV was obtained experimentally [15] and theoretically [16], and we have found the ESD for Na atoms from adsorbed Na and Au layers on W at a coverage of more than 1 ML.

The aim of the present work is to check the semiconductor film formation by means of the ESD for Cs atoms from cesium layers adsorbed on gold-covered tungsten, to measure the ESD yield and energy distribution (ED) for Cs atoms from cesium layers adsorbed on gold-film-covered tungsten surfaces as a function of cesium coverage, gold film thickness, bombardment electron energy and substrate temperature, as well as to discuss the nature of physical processes leading to the surface layer destruction by electron beam.

2. Experimental details

The experimental set-up and procedure used in the sample preparation for measurements are described in detail elsewhere [17]. In brief, the measurements are carried out in a bakeable stainless-steel chamber with a residual gas pressure below 5×10^{-10} Torr. The ESD energy distributions for Cs atoms are measured by means of a time-of-flight method by pulsing the electron beam using gating pulses of duration 1 μs and repetition frequency 1 kHz. The electron current density does not exceed 10^{-6} A cm^{-2} at electron energy $E_e = 200$ eV, so there is no noticeable heating of the sample. The flux of desorbing positive ions is retarded by the potential between the target and the screen electrode arranged in the drift space. The neutral particles are ionized in a surface ionization detector consisting of a textured tungsten ribbon heated to $T = 1800$ K and the ion current signal is amplified by a secondary electron multiplier.

A textured tungsten ribbon measuring $70 \times 2 \times 0.01$ mm^3 with a predominantly (100)-oriented surface is used as the target. To produce a predominantly (100)-oriented surface the ribbon is heated in ultrahigh vacuum at $T = 2000$ K for 5 h by an alternating current. It consists of crystalline blocks with (100) oriented surface and has an average block size of 20 μm determined by scanning electron spectroscopy [18]. The sample contamination is checked using Auger electron spectroscopy, work function measurements and thermal desorption. In a separate experiment gold is deposited onto the ribbon at $T = 300$ K from a directly heated tungsten tube containing gold pieces of 99.99% purity. The tube has several holes to provide a uniform gold desorption rate along the sample. The concentration of deposited gold is determined from the deposition time under constant gold flux and is checked by means of the total sodium current during surface ionization at the sample surface fully covered with gold. Oxygen is not adsorbed on gold at $T = 300$ K but increases the work function of tungsten. The sample is cleaned of carbon by annealing in an oxygen atmosphere $p(O_2) = 1 \times 10^{-6}$ Torr at $T = 1800$ K for 3 h.

Cesium is deposited onto the ribbon at $T = 300$ K from a directly heated evaporator by thermal decomposition of the cesium chromate. The concentration of deposited cesium is determined from the deposition time under constant cesium flux. The cesium flux intensity is measured by means of the total cesium current during surface ionization at the sample surface heated to the current saturation temperature [19].

The sample can be cooled by flowing gaseous nitrogen through the hollow current leads via a copper pipe immersed in liquid nitrogen. The sample temperature is varied in the temperature range 160–300 K by changing the gas flow rate and temperature measurements in this range are based on the sample resistance. In addition, the sample can be heated resistively and the sample temperature is determined with an optical micropyrometer in the high-temperature range. A linear extrapolation of the temperature dependence of the heating current is used to determined temperatures between 300 K and incandescence.

3. Results

Electron bombardment of a cesium layer adsorbed on gold-covered tungsten results in desorption of Cs atoms. Figure 1 shows a plot of the ESD yield for Cs atoms from a cesium layer adsorbed on a two monolayer (ML) gold-covered tungsten surface at a substrate temperature of 300 K and at an electron energy of 64 eV. The bombardment electron energy of 64 eV is chosen because the ESD yield for Cs atoms as a function of electron energy has a maximum at 64 eV and at these conditions. The Cs atom ESD yield appears at a Cs concentration of 5×10^{14} at cm^{-2} which corresponds to the formation of 1 ML. It grows linearly with the Cs concentration, reaching saturation at two Cs monolayers. Apparently, the first Cs monolayer corresponds to the formation of Cs film with metallic properties in which excitation lifetime is too small for the Cs atom to be desorbed. But, following Cs monolayer formation on the Au surface, the
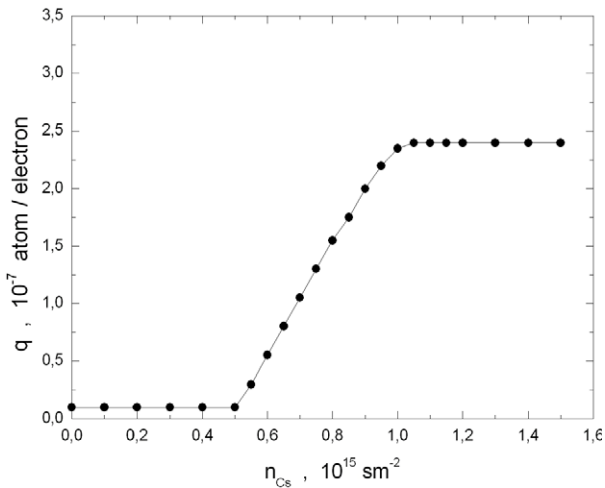
Figure 1. ESD yield for Cs atoms from a Cs layer adsorbed on 2 ML gold-covered tungsten at temperature $T = 300$ K as a function of adsorbed Cs concentration measured at an electron energy of 64 eV and at temperature $T = 300$ K.
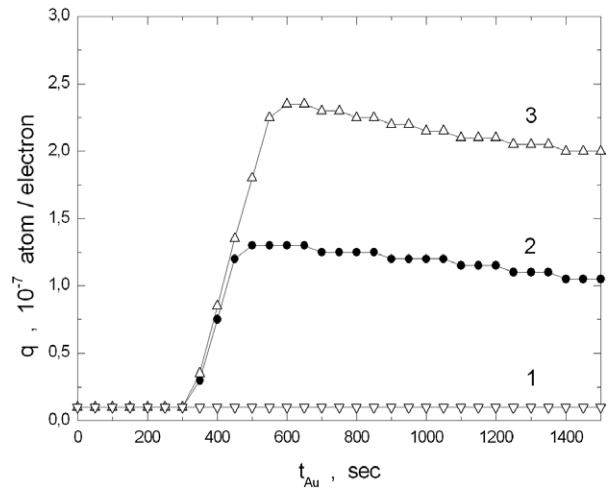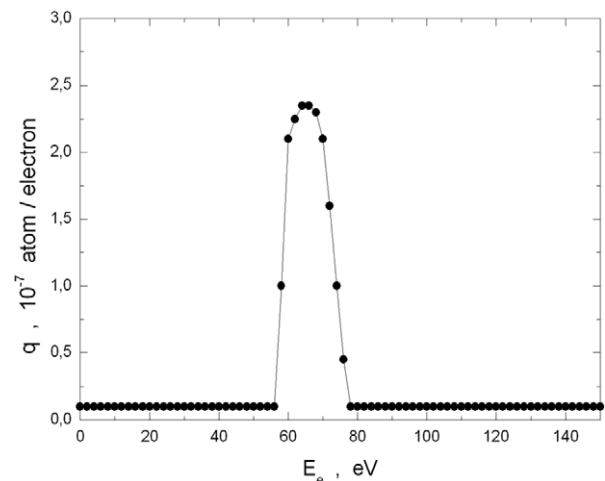

Figure 2. ESD yield for Cs atoms from Cs layers with different Cs concentrations adsorbed on substrate as a function of Au deposition time deposited on tungsten and measured at $E_e = 64$ eV and at $T = 300$ K: 1–0.5 × 10^{15} at cm^{-2}, 2–0.75 × 10^{15} at cm^{-2} and 3–1.0 × 10^{15} at cm^{-2}.

CsAu semiconductor compound starts to grow in which the excitation state lifetime is expected to be much greater. This is supported by an electrical resistance increase in Cs deposition after the monolayer formation.

The system consists of different patches: Cs monolayer on the Au/W metal-film surface and Cs monolayer on the CsAu semiconductor alloy surface. The ESD for Cs atoms occurs only from the Cs monolayer adsorbed on the semiconductor patches. The Cs atom ESD yield grows linearly with increasing CsAu semiconductor film area up to $n_{Cs} \sim 1 \times 10^{15}$ at cm^{-2} and does not depend on the following Cs exposure (figure 1). That insensitivity to higher Cs exposure might be due to the absence of Cs adsorption on the Cs monolayer surface [15].

The similar plot to figure 1 for the ESD yield of Na atoms as a function of sodium concentration passes through a maximum around $\Theta = 2$ that is due to continuous growth of the Na film. The ESD yield for Cs atoms reaches saturation with increasing Cs concentration, but does not pass through a maximum since Cs does not adsorb above a monolayer on this surface at $T = 300$ K [20]. These Cs monolayer formation features on a CsAu alloy film-covered tungsten surface are supported by figure 2 which presents plots of the Cs atom ESD yield versus gold deposition time for different Cs concentrations deposited at $T = 300$ K and measured at an electron energy of 64 eV. The Cs atom ESD yield appearance time ($t_{Au} = 300$ s) corresponds to an Au monolayer formation with over a ML of Cs on top. The Cs atom ESD yield grows linearly with increasing Au deposition time, reaching a maximum after the deposition of two Cs and Au monolayers ($t_{Au} = 600$ s). Note that, in order for the Cs atom yield results to be reproduced, each point in figure 2 is measured from a new portion of Cs deposited onto a corresponding Au film. Hence, Cs is always deposited on top of Au. An insignificant Cs atom yield drop is seen with increasing adsorbed Au film on W (with increasing t_{Au}) that can be caused by Cs diffusion into the Au thick film.
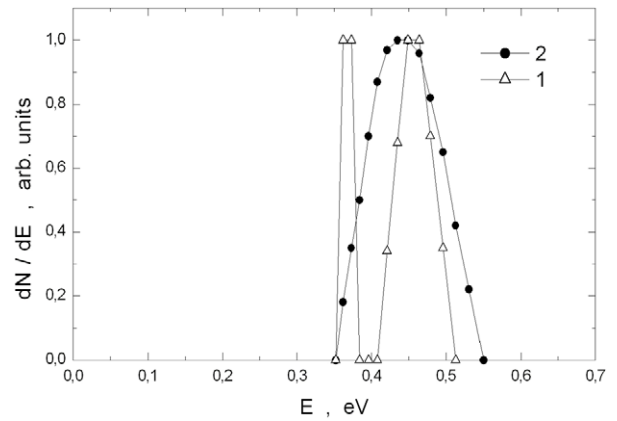

Figure 3. ESD yield for Cs atoms from a Cs layer with a concentration of 1.0×10^{15} at cm^{-2} adsorbed on 2 ML gold-covered tungsten as a function of electron energy at $T = 300$ K.

The dependence of the ESD yield for Cs atom on electron energy (figure 3) has a resonant character with a maximum at an electron energy of 64 eV which is close to the Au 5p shell energy (57–75 eV) [21]. The Cs atom yield peak has a slightly asymmetric shape extended toward high energies. This plot differs substantially from one of the Na atom yield which has two maxima at electron energies of 64 and 82 eV, close to the core level energies of the Au 5p$_{3/2}$ (57 eV) and Au 5p$_{1/2}$ (75 eV) [21].

Figure 4 displays plots of the normalized Cs atom ESD energy distributions for three Cs concentrations adsorbed on a 2 ML gold-covered tungsten surface measured at $T = 300$ K and at an electron energy of 64 eV. These EDs have a bell-shaped form with a maximum at a kinetic energy of $\sim$0.5 eV at $T = 300$ K and at a Cs concentration of 0.6×10^{15} at cm^{-2} which are shifted toward lower energies with increasing Cs
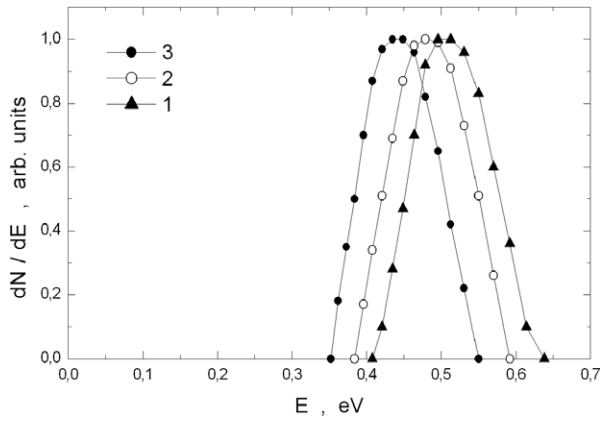
Figure 4. Normalized ESD energy distribution for Cs atoms from a Cs layer with different Cs concentrations adsorbed on 2 ML gold-covered tungsten measured at $E_e = 64$ eV and $T = 300$ K: 1—0.6×10^{15} at cm^{-2}, 2—0.75×10^{15} at cm^{-2} and 3—1.0×10^{15} at cm^{-2}.

Figure 6. Normalized ESD energy distribution for Cs atoms from a Cs layer adsorbed at $T = 300$ K on 2 ML gold-covered tungsten measured at $T = 160$ K (curve 1) and 300 K (curve 2) and at $E_e = 64$ eV.
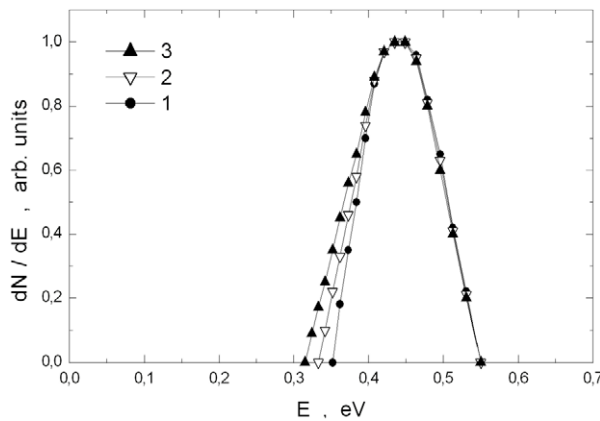
Figure 5. Normalized ESD energy distribution for Cs atoms from a Cs layer adsorbed on different deposition time gold-covered tungsten and measured at $E_e = 64$ eV and $T = 300$ K: 1—600 s, 2—900 s, 3—1200 s.
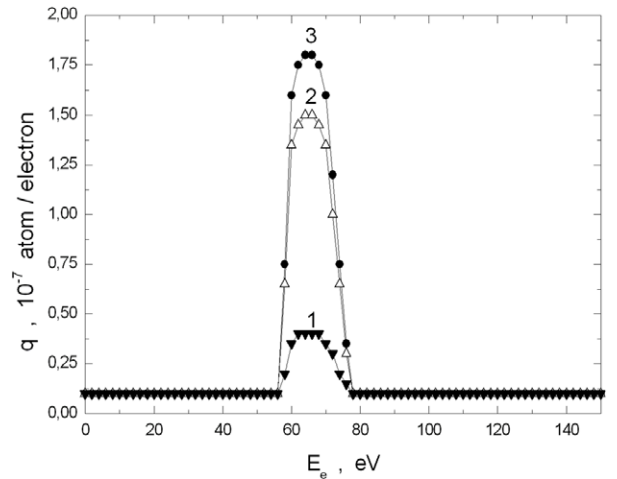
Figure 7. ESD yield for Cs atoms from a Cs layer with a Cs concentration of 1.0×10^{15} at cm^{-2} adsorbed at $T = 300$ K on 2 ML gold-covered tungsten as a function of electron energy measured at $T = 160$ K. Yield for LE peak—curve 1, yield for HE peak—curve 2 and the total yield—curve 3.

concentration without any shape change. The ED for Cs atoms differs noticeably from the ED for Na atoms which consists of two peaks at $T = 300$ K: a broad peak with a maximum at ~ 0.35 eV and a narrow peak with a maximum at ~ 0.15 eV [13].

Figure 5 presents plots of the normalized Cs atom ESD energy distributions for three different Au films deposited on a tungsten substrate covered by a Cs film with a concentration of 1.0×10^{15} at cm^{-2} and measured at an electron energy of 64 eV. The EDs are bell-shaped with a maximum at 0.45 eV. The ED front shifts toward lower energies with increasing Au concentration but the ED tail position is independent of Au concentration.

When T decreases below 240 K, the ESD yield for Cs atoms appears in the cesium surface concentration range 0.55–0.65×10^{15} at cm^{-2} at the energies of incident electrons from 24 to 50 eV with a maximum between 32 and 44 eV. Simultaneously a new peak emerges in the energy distribution of Cs atoms with a maximum at 0.57 eV.

Figure 6 shows the transformation of the normalized Cs atom ESD energy distribution with changing temperature from 300 to 160 K for a tungsten surface covered by two Au and Cs monolayers. The ESD yield for Cs atoms associated with the appearance threshold of 24 eV is observed only at $T < 240$ K. The ED with a single peak is converted into the ED with two peaks: the broad, high-energy (HE) peak with a maximum at a kinetic energy of 0.46 eV and the narrow, low-energy (LE) peak with a maximum at a kinetic energy of 0.36 eV.

Figure 7 displays plots of the Cs atom ESD yield for HE and LE peaks as well as the total Cs atom ESD yield at $T = 160$ K as a function of electron energy from Cs layers adsorbed on 2 ML gold-covered tungsten. The HE peak intensity is about five times greater than the intensity of the LE peak.

Figure 8 shows the normalized Cs atom ESD energy distribution for two Cs concentrations of 0.75×10^{15} and
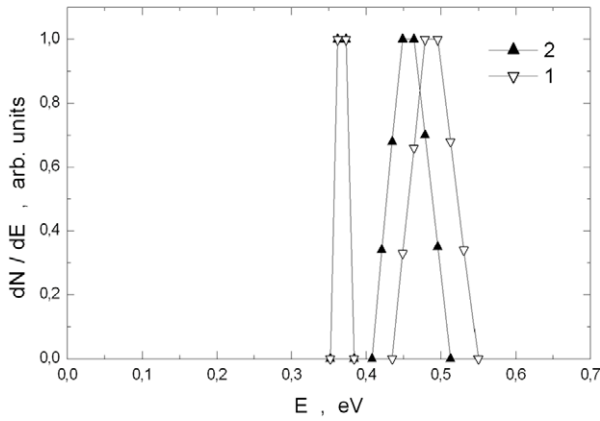
Figure 8. Normalized ESD energy distribution for Cs atoms from a Cs layer with Cs concentrations of 0.75×10^{15} at cm^{-2} (curve 1) and 1.0×10^{15} at cm^{-2} (curve 2) adsorbed on 2 ML gold-covered tungsten at $T = 300$ K measured at $E_e = 64$ eV and at $T = 160$ K.
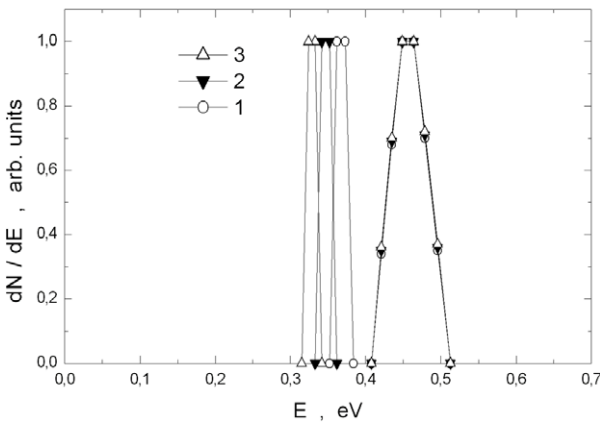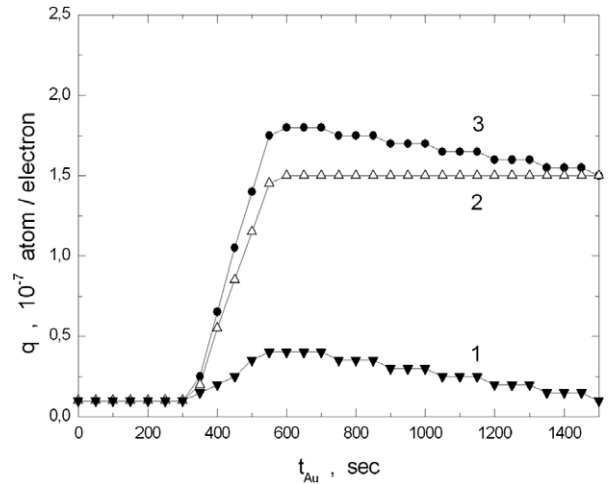

Figure 9. Normalized ESD energy distribution for Cs atoms from a Cs layer with a Cs concentration of 1.0×10^{15} at cm^{-2} adsorbed on different deposition time gold-covered tungsten at $T = 300$ K measured at $E_e = 64$ eV and $T = 160$ K: 1–600 s, 2–900 s and 3–1200 s.

Figure 10. ESD yield of Cs atoms from a Cs layer with a Cs concentration of 1.0×10^{15} at cm^{-2} adsorbed on gold-covered tungsten at $T = 300$ K as a function of Au deposition time measured at $E_e = 64$ eV and $T = 160$ K. Yield for LE peak—curve 1, yield for HE peak—curve 2 and the total yield—curve 3.
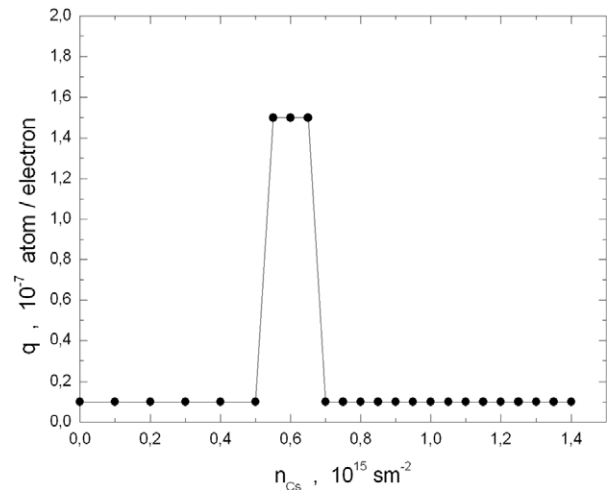
Figure 11. ESD yield for Cs atoms from a Cs layer adsorbed on 2 ML gold-covered tungsten at $T = 300$ K as a function of adsorbed Cs concentration measured at $E_e = 38$ eV and at $T = 160$ K.

1.0×10^{15} at cm^{-2} adsorbed on 2 ML gold-covered tungsten measured at an electron energy of 64 eV and at a substrate temperature of 160 K. The LE peak preserves its position on the energy scale, but the HE peak shifts toward low energies without any shape change with increasing Cs concentration.

Figure 9 presents the normalized Cs atom ESD energy distribution for a Cs concentration of 1.0×10^{15} at cm^{-2} adsorbed on different gold-concentration-covered tungsten surfaces and measured at a substrate temperature of 160 K and at an electron energy of 64 eV. Contrary to figure 8 the HE peak position on the energy scale persists and the LE peak shifts toward lower energies with growing Au concentration.

Figure 10 shows that the HE peak intensity is independent of the Au film thickness and the LE peak intensity decreases gradually with Au film growth.

Figure 11 displays the Cs atom ESD yield plotted versus the Cs concentration adsorbed on 2 ML gold-covered tungsten at a substrate temperature of 300 K and measured at an electron energy of 38 eV and $T = 160$ K. The bombardment electron

energy of 38 eV is chosen because the ESD yield for Cs atoms as a function of electron energy has a maximum at 38 eV and at these conditions. The desorption flux appears after 1 ML cesium adsorption, approaches a maximum at a Cs concentration of 0.6×10^{15} at cm^{-2} and then goes to zero at a Cs concentration of 0.7×10^{15} at cm^{-2}.

Figure 12 compares the dependences of the Na atom ESD yield with the Cs atom ESD yield as a function of electron energy at $T = 160$ K and at alkali metal coverages close to an ML. In both cases the ESD yield depends resonantly on the electron energy. The Na atom yield appears at an electron energy of $\sim$30 eV, reaches the first maximum at $\sim$40 eV, goes to zero at $\sim$55 eV and passes through maxima at electron energies of 64 and 82 eV [13]. The Cs atom yield in the first maximum is shifted toward lower energies by 6 eV, the threshold for the second maximum is the same as for the Na
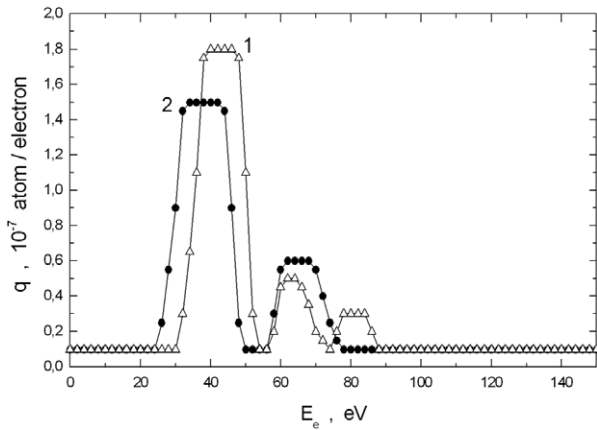
Figure 12. ESD yield for Na or Cs atoms from Na or Cs layers adsorbed on 2 ML gold-covered tungsten at $T = 300$ K as a function of electron energy measured at Na 1.0×10^{15} at cm^{-2} (curve 1) or Cs 0.65×10^{15} at cm^{-2} (curve 2) concentrations and at $T = 160$ K.
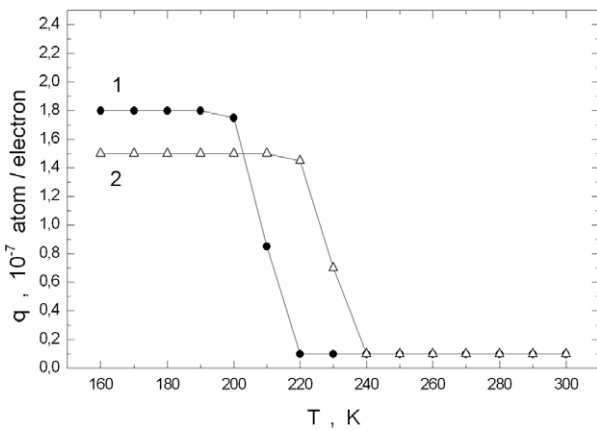

Figure 13. ESD yield for Na (curve 1) or Cs (curve 2) atoms from Na or Cs layers adsorbed on 2 ML gold-covered tungsten at $T = 300$ K as a function of substrate temperature.

atom yield and the third maximum is unresolved and merges the second peak. Its presence broadens the second maximum in comparison with the Na atom yield maximum width.

Figure 13 compares the temperature dependences of the Na and Cs atom ESD yields at coverages close to an ML, adsorbed on 2 ML gold-covered tungsten and measured at $E_e = 38$ eV for Cs atoms and at $E_e = 44$ eV for Na atoms. The bombardment electron energies of 38 and 44 eV are chosen because the Cs and Na atom ESD yields as a function of electron energy have maxima at 38 and 44 eV, correspondingly, and at these conditions. The Na atom yield does not depend on the temperature up to $T = 200$ K and then goes to zero within the temperature range of 20 K. The Cs atom yield is independent of temperature up to $T = 220$ K and then drops to zero too.

Figure 14 shows the normalized Cs atom ESD energy distributions for a Cs concentration of 0.65×10^{15} at cm^{-2} deposited on 2 ML gold-covered tungsten at a temperature of 160 K and measured at electron energies of 38 and 64 eV. In the first case, the Cs 5s level is excited and, in the second case,
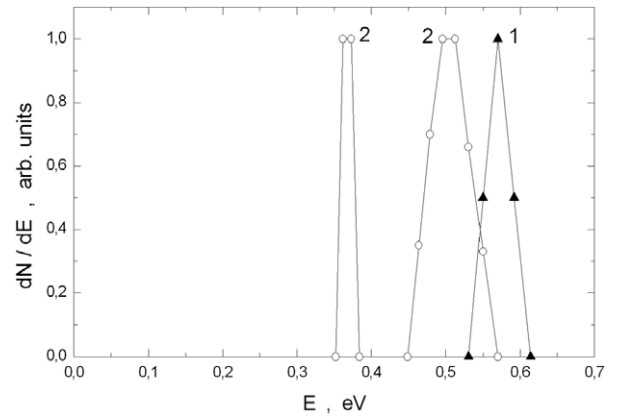
Figure 14. Normalized ESD energy distribution for Cs atoms from Cs layers adsorbed at $T = 300$ K on 2 ML gold-covered tungsten measured at $T = 160$ K and at a Cs concentration of 0.65×10^{15} at cm^{-2} and for two electron energies of 38 eV (curve 1) and 64 eV (curve 2).

the Au substrate $5p_{3/2}$ level is excited, which are responsible for the formation of HE and LE peaks in the Cs atom energy distribution, respectively. The Cs atom peak position after the excitation of the Cs 5s level corresponds to the Na atom peak position in the Na atom energy distribution after the excitation of the Na 2p level at the adsorption of 0.9×10^{15} at cm^{-2} sodium on 2 ML gold-covered tungsten at $T = 160$ K.

4. Discussion

The solubility of gold in tungsten is negligible and so the gold–tungsten interface is atomically sharp. Moreover, for coverage less than a monolayer gold grows epitaxially on the W(100) face. Above that coverage it forms misoriented crystals with bulk properties [22, 23]. The deposition of Cs on gold-covered tungsten is accompanied by the reduction of work function [16, 24]. The two phases are observed in thermodesorption of Cs from the Cs-1 ML Au–W adsorption system, one of which is saturated and attributed to the Cs monolayer completion, whereas the second phase exhibits unsaturated growth and correlates with the formation of a semiconductor $Cs_x Au_y$ compound [25].

Cesium adsorbs on 1 ML gold-covered tungsten at room temperature up to a monolayer saturation coverage and does not react with gold to form a compound. This system possesses metallic properties as any metal-film covered substrate has an excited state lifetime not long enough to produce ESD. To start the reaction it is necessary to exceed monolayer concentrations both for gold and cesium. Deposition of Cs on 2 ML gold film results in the formation of the following system: a monolayer of gold on tungsten covered with $Cs_x Au_y$ compound and a monolayer of Cs over it. The compound film exhibits semiconductor properties [15, 16] and provides the greater excited state lifetime.

The amount of Cs adsorbed on gold-covered tungsten is restricted to the number of Cs anions forming the $Cs_x Au_y$ compound and a monolayer coverage over it. Cs is not adsorbed on top of a cesium monolayer at room temperature,
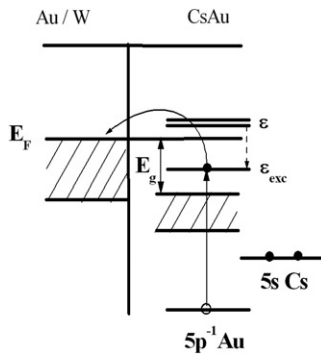
Figure 15. Schematic potential diagram for electronic transitions in Cs atom ESD for core level excitations. E_g—forbidden band.

so the Cs atom yield reaches saturation with increasing cesium concentration (figure 1). It is not the case for sodium that can form a multilayer Na film over the Na_xAu_y compound, so the ESD yield for Na atoms passes through a maximum with increasing sodium concentration [13] due to gold screening by Na atoms.

Apparently the resonant Cs atom yield (figure 3) is associated with the excitation of $5p_{3/2}$ Au electrons to the peaks of an unoccupied conduction band (CB) density of states in the range of 57–78 eV that is accompanied by the formation of core exciton $5p^{-1}$ Au-ε_{exc} in which the excited state of the conduction band ε_{exc} is localized by the hole field.

Indeed, as the calculations show, these peaks appear in the CB on a metal or semiconductor surface after the adsorption of alkali metals [26–28]. These peaks above the Fermi level E_F are formed by the hybridization of adsorbed alkali-metal atom and surface electron orbitals and give antibonding states [26]. These states fall lower than the conduction band bottom due to the hole field but their electrons may go over to the conduction band. Such two-stage core level excitation has a much greater probability than the direct ionization [10] that can explain a purely resonant ESD yield dependence as a function of electron energy. The desorption of Cs atoms arises only from the patches where there is the Cs_xAu_y compound under the Cs monolayer that increases the excited antibonding state lifetime in comparison with the one on the Au/W metal patches. The scheme of electron processes in the ESD for Cs atoms is given in figure 15.

The hole in the Au $5p_{3/2}$ level created by this excitation can be filled by an electron from a higher-energy level via an Auger decay process. The electrons arising from hole Auger neutralization occur in the conduction band. The slow electrons near the Fermi level can be captured by either a Cs^+ ion adsorbed in the monolayer or a molecule CsAu, forming the alloy. The capture of the electrons by the adsorbed Cs^+ ions results in their neutralization and desorption. The capture of an electron from the CB by a Cs^+Au^- molecule, forming the alloy, transfers it to an antibonding state. The bond of the Cs^+Au^- molecule in the alloy is destroyed and the Cs atom escapes from the alloy. This process is similar to the destruction of the CsAu alloy in the photon irradiation with $h\nu > 2.6$ eV [29] and to the dissociative electron attachment.

Note that the resonant dependence of the ESD yield for Cs atoms on electron energy may arise only from the excitation of the substrate or adsorbed layer by electrons in strong localized states, rather than from simple ionization with the formation of free electrons whose probability has a smooth dependence on electron energy and its value is less than the excitation probability in the localized states [30–32]. The existence of density state peaks in the CB is an indispensable condition for the appearance of the ESD yield resonances. The absence of any high-energy tails in a resonant spectrum $q(E_e)$ means that secondary electrons do not take part in the Cs atom ESD and the spectrum is formed by 5p Au core electron excitation and by the capture of conductivity electrons by either an adsorbed Cs atom or a CsAu molecule, forming the alloy.

The Na atom ESD yield from a sodium layer adsorbed on gold-covered tungsten plotted versus electron energy has two resonant peaks associated with the exciton state excitations of Au $5p_{3/2}$ and $5p_{1/2}$ levels, whose energies are close to the appearance thresholds of these resonances. However, the ESD yield for Cs atoms from a cesium layer adsorbed on gold-covered tungsten as a function of electron energy has only one resonance (figure 3), whose appearance threshold coincides with the Au $5p_{3/2}$ level energy. The Au $5p_{1/2}$ level excitation is assumed to be quenched by a Cs $4d_{5/2}$ level resonance in the surrounding Cs atoms. As a result of this process, the state at an energy of 75 eV partly delocalizes and the probability of its excitation reduces, extending the Au $5p_{3/2}$ resonance peak.

The ESD energy distribution for Cs atoms is a bell-shaped curve at $T = 300$ K and $E_e = 64$ eV with a maximum which shifts toward lower energies with increasing Cs coverage from 0.6 to 1 (figure 4). Such a displacement of the Cs atom ESD energy distribution with increasing Cs coverage depositing over the monolayer on a heterogeneous surface with patches of Au/W and CsAu/W may be explained by the supposition that the distance between the Cs monolayer and the surface increases and the adsorbed atom repulsion from the surface decreases.

Such ED behavior with growing Cs coverage can serve as an additional indication of the broad peak origin in the ESD energy distribution for Cs atoms by analogy with the Na atom ESD energy distribution from the Na/NaAu/W system [13]. There is a narrow peak ($E_{max} = 0.15$ eV) besides a broad peak ($E_{max} = 0.35$ eV) for the Na atom ESD energy distribution from the NaAu alloy, but there is no narrow peak in the Cs atom ESD ED at $T = 300$ K (figure 4). However, the broad peak in the ESD energy distribution for Cs atoms expands and the leading edge of ED shifts toward lower energies with increasing Au deposition time (figure 5). It is possible that the left ED wing arises from an ESD channel that is different from that causing the right ED wing and the Cs atom ED peak is composite. Indeed, the surface cooling to 160 K (figure 6) allows us to separate the broad HE peak in the ESD energy distribution for Cs atoms into two peaks: the narrow LE peak with a maximum at 0.37 eV and the broad HE peak with a maximum at 0.45 eV. The separation between them is less than that in the paper [13] for the ESD energy distribution of Na atoms ($\Delta E_{Na} \approx 0.2$ eV). Figure 7 shows that the LE peak intensity is 4–5 times less than the HE peak intensity. When the temperature increases the peaks are extended and merged.

Figures 8–10 can support our interpretation of the HE and LE peak formation mechanisms in the energy distribution for alkali-metal atoms at $E_e = 64$ eV in the paper [13]: the LE peak is formed by alkali-metal atoms arising from the destroyed alloy CsAu or NaAu layers and the HE peak is formed by adsorbed alkali-metal atoms on the alloy surface. Both peaks result from the same process of Au 5p level excitation in the CB 'resonances', but the conduction band electrons arising from the excited state decay or Auger neutralization of Au 5p holes can be captured in different antibonding states that give either the broad HE peak in the ED for alkali-metal atoms or the narrow LE peak in the ED for CsAu molecules. Indeed, the HE peak intensity depends on the adsorbed Cs concentration and the LE peak intensity does not depend on it (figure 8). The broad HE peak in the Cs atom ESD energy distribution does not change, but the narrow LE peak shifts toward lower energies with increasing Au deposition time at $T = 160$ K (figure 9). The HE peak intensity does not depend on the Au layer thickness, while the LE peak intensity does, shifting toward lower energies and decreasing the ESD yield for Cs atoms with Au deposition time (figure 10). Apparently the LE peak yield attenuation is caused by cesium diffusion from a top alloy layer and a depletion of its concentration. It is possible that the LE peak intensity decrease in the ESD energy distribution for Na atoms is more noticeable (figure 4 [13]) because of the greater mobility of sodium in the NaAu layer.

The decrease of the substrate temperature from 300 to 160 K in the measurements of the ESD for Cs atoms enables us to observe additional resonance in the ESD yield $q(E_e)$ with a threshold around 24 eV and a maximum at 40 eV (figure 12), similar to $q(E_e)$ for Na atoms [14]. The appearance of this resonance can be explained by the excitation of adatom core shells (Cs 5s and Na 2p in the paper [13]). The desorption mechanism in such an excitation of an adatom core exciton is put forward in the paper [14]. The excitation of an adatom core level creates an exciton on the adatom (figure 15). The decay of this exciton transfers the exciton electron to the conduction band and the Cs^+ ion turns into a Cs^{2+} ion which starts moving toward the surface due to an increase in the image force and a decrease in repulsion between the Cs^{2+} ion and the surface [33]. Its neutralization and repulsion from the surface occur at a distance which is closer to the surface than the equilibrium cesium monolayer distance so the desorbing atom in this channel acquires a greater kinetic energy than in atom ESD from a cesium monolayer after the excitation of a 5p Au level. The shape and position of ED for Cs atoms do not depend on the adsorbed cesium concentration in this channel. This is additional evidence of the Cs^{2+} ion formation and its reverse motion because the Cs^{2+} ions are neutralized at the same distance which is very close to the surface and independent of their velocity.

But the probability of Cs^{2+} ion formation in transmission with a local exciton level to the conduction band exponentially decreases with increasing distance between cesium and the substrate. So the ESD yield for Cs atoms decreases sharply with increasing temperature and semiconductor CsAu patch area under the Cs monolayer in this channel (figures 11

and 13). The Cs atom ESD yield exists only in the narrow cesium coverage range (figure 11) appearing after the formation of the semiconductor alloy layer at $\Theta_{Cs} \geqslant 1$. Its intensity vanishes at $n_{Cs} \sim 7 \times 10^{14}$ at cm^{-2}, i.e. at a semiconductor layer area exceeding ~40% of the monolayer.

The sharp ESD yield drop with increasing temperature (figure 13) in the reverse motion channel has been observed earlier in the Eu or Sm atom ESD from Eu or Sm layers adsorbed on oxidized tungsten [31]. We conclude that all the process probabilities, that affect the ESD yield of neutral particles in this channel, have a stronger temperature dependence than the probabilities of the same processes in the excitation of substrate atoms, Au [13] and W [31]. Since the adsorbed atom vibrations are anharmonic, their amplitudes and distances from the surface are very sensitive to temperature, whereas the vibrations of substrate atoms are close to harmonic and their properties in the bulk are almost independent of T.

5. Conclusion

(1) The ESD yield for Cs atoms from the Cs/Au/W substrate exists only at a coverage of Au and Cs greater than a monolayer.

(2) The resonant character of the Cs atom ESD yield often testifies to the formation of a core exciton in which the excited electron is localized by the hole field. The resonance with a maximum of 64 eV is associated with the Au 5p level substrate excitation. The second resonance with a maximum of ~40 eV appears at $T < 240$ K and exists only at a low Cs coverage. It is due to the Cs 5s level excitation in the adsorbed Cs ion.

(3) The Au $5p_{1/2}$ level excitation which is well seen in the ESD for Na atoms from Na layers adsorbed on gold-covered tungsten is quenched in the given case because of resonance electron transition from the Cs $4d_{5/2}$ level.

(4) The Au $5p_{3/2}$ level excitation leads to two Cs atom ESD mechanisms which correspond to different peaks in the energy distribution of Cs atoms at $T = 160$ K: the broad HE peak is formed by Cs atoms from the Cs adsorbed layer and the narrow LE peak is formed by Cs atoms from the CsAu alloy destruction under electron bombardment.

(5) The resonant dependence of the Cs atom ESD yield results from the excitation of core electrons of the adsorbed layer or substrate atoms in the density of state CB peaks, rather than from simple core electron ionization.

Acknowledgments

References

[1] Ageev V N 1994 *Prog. Surf. Sci.* **47** 55
[2] Madey T E 1994 *Surf. Sci.* **299/300** 824
[3] Ramsier R D and Yates J T 1991 *Surf. Sci. Rep.* **12** 247

[4] Yakshinskiy B V and Madey T E 2003 *Surf. Sci.* **528** 54
[5] Ageev V N, Kuznetsov Yu A and Potekhina N D 1996 *Surf. Sci.* **367** 113
[6] Ageev V N, Kuznetsov Yu A and Potekhina N D 1997 *Phys. Solid State* **39** 671
[7] Ageev V N, Kuznetsov Yu A and Madey T E 1997 *Surf. Sci.* **390** 146
[8] Ageev V N, Kuznetsov Yu A and Madey T E 1998 *Phys. Rev. B* **58** 2248
[9] Ageev V N, Kuznetsov Yu A and Madey T E 2003 *J. Electron. Spectrosc.* **128** 223
[10] Ageev V N, Kuznetsov Yu A and Potekhina N D 2003 *Phys. Solid State* **45** 976
[11] Ageev V N, Kuznetsov Yu A and Madey T E 2006 *Surf. Sci.* **600** 2163
[12] Ageev V N, Kuznetsov Yu A and Madey T E 2007 *J. Vac. Sci. Technol.* A **25** 731
[13] Ageev V N, Kuznetsov Yu A and Potekhina N D 2008 *Phys. Solid State* **50** 1585
[14] Ageev V N, Kuznetsov Yu A and Potekhina N D 2009 *Phys. Solid State* **51** 417
[15] Skottke-Klein M, Böttcher A, Imbeck R, Kennou S, Morgante A and Ertl G 1991 *Thin Solid Films* **203** 131
[16] Koenig C, Christensen N E and Kollar J 1984 *Phys. Rev. B* **29** 6481
[17] Ageev V N, Burmistrova O P and Kuznetsov Yu A 1987 *Sov. Phys.—Solid State* **29** 1000
[18] Potekhina N D, Gall' N R, Rut'kov E V and Tontegode A Ya 2003 *Phys. Solid State* **45** 782
[19] Zandberg E Ya and Ionov N I 1969 *Poverkhnostnaya Ionizatsiya* (Moscow: Nauka) (in Russian)
[20] Ageev V N, Ionov N I, Medvedev B K and Yakshinskii B V 1978 *Sov. Phys.—Solid State* **20** 767
[21] Briggs D and Seah M P 1990 *Practical Surface Analysis* (*Auger and X-Ray Photoelectron Spectroscopy* vol 1) 2nd edn (Chichester: Wiley)
[22] Bauer E, Boncerek T, Poppa H and Todd G 1975 *Surf. Sci.* **53** 87
[23] Wertheim G K, Buchanan D N E and Lee V 1986 *Phys. Rev. B* **34** 6869
[24] Knat'ko M V, Lapushkin M N and Paleev V I 1998 *Tech. Phys. Lett.* **24** 390
[25] Ageev V N and Afanas'eva E Yu 2006 *Phys. Solid State* **48** 2347
[26] Wimmer E 1983 *J. Phys. F: Met. Phys.* **13** 2313
[27] Ishida H 1988 *Phys. Rev. B* **38** 8006
[28] Soukiassian P, Bakshi M H, Hurych Z and Gentle T M 1989 *Surf. Sci.* **221** L759
[29] Knat'ko M V, Lapushkin M N and Paleev V I 1998 *Tech. Phys.* **43** 1235
[30] Mori A, Kayanuma Y and Kotani A 1991 *Prog. Theor. Phys. Suppl.* **106** 75
[31] Ageev V N, Kuznetsov Yu A and Potekhina N D 2004 *Phys. Solid State* **46** 975
[32] Ageev V N, Kuznetsov Yu A and Potekhina N D 2007 *Phys. Solid State* **49** 1589
[33] Antoniewicz P R 1980 *Phys. Rev. B* **21** 3811